Supplementary information

Supplementary Figure 1. gp96 forms complex with AIMP1 independent of tRNA synthetase complex. The proteins extracted from HL-60 cells were immunoprecipitated with control IgG, anti-gp96 antibody, or anti-EPRS antibody, and the precipitated proteins were immunoblotted with anti-EPRS, anti-p43, or anti-gp96 antibody. The data shown are representative of three separate experiments.

Supplementary Figure 2. Deletion of E791 of gp96 decrease AIMP1 binding. (A) gp96 WT and E791Δspanning aa 289-799 were expressed as GST fusion protein in *E. coli*. The purified gp96 proteins were incubated with mock or AIMP1, and the co-precipitation of AIMP1 were determined by immunoblotting with anti-AIMP1 antibody. (B) The effect of gp96 variant E791Δ on AIMP1 binding. gp96 WT and E791Δ were expressed as His fusion protein in *E. coli*. The purified gp96 proteins were incubated with GST or GST-AIMP1, and the co-precipitation of gp96 was determined by immunoblotting with anti-gp96 antibody. Data shown are the representative result of three independent experiments.

Supplementary Figure 3. Interaction of AIMP1 with KDELR1. The 1-53 aa, 54-192

aa, and 193-312 aa peptides of AIMP1 were expressed as GST fusion proteins in *E.coli*. The purified GST-fused AIMP1 fragments were incubated with HeLa cell lysates and the co-precipitation of KDELR1 was determined by immunoblotting with anti-KDELR1 antibody. The data shown are representative of three separate experiments.

Supplementary Figure 4. Surface localization of gp96 in AIMP1-deficeint cells. Bone marrow cells from AIMP1$^{+/+}$ (dotted line) and AIMP1$^{-/-}$ (solid line) mice were stained for cell surface gp96, along with other lineage-specific markers, followed by flow cytometry analysis. Gp96^{+} cells from AIMP1$^{-/-}$ and AIMP1$^{+/+}$ mice were 55% vs. 42% in B220^{+} populations; 7.1% vs. 3.4% in CD11b^{+} populations; 4.6% vs. 2.9% in Gr-1^{+} populations. The data shown are representative of three separate experiments.

Supplementary Figure 5. Activation of dendritic cells in AIMP1-deficient mice. Splenic CD11c^{+} cells from AIMP1$^{+/+}$ or AIMP1$^{-/-}$ mice (n=3) were analyzed by flow cytometry for the expression of CD80, OX40L, CD83, and MHC class II on the cell surfaces. Shown are the representative data from one mouse in each group and the percentages of maturation marker^{+}/CD11c(high) cells are indicated.

Supplementary Figure 6. T cell and regulatory T cell development in AIMP1$^{-/-}$ cells.

(A) Thymocytes and splenocytes from AIMP1$^{+/+}$ or AIMP1$^{-/-}$ mice (n=3) were analyzed by flow cytometry for the expression of CD4 and CD8 on the cell surfaces. (B) Thymocytes from AIMP1$^{+/+}$ or AIMP1$^{-/-}$ mice (n=3) were analyzed by flow cytometry for the expression of CD4 and CD44 on the cell surfaces. (C) WT or AIMP1$^{-/-}$ thymocytes from 11 weeks old mice were separated into CD4^{+} or CD4^{-} cells. For the determination of the expression of Foxp3 (regulatory T cell marker) and HPRT (hypoxanthine-guanine phosphoribosyl-transferase: control), we carried out semi-quantitative RT-PCR using primers as previously described[60]. We isolated the total RNAs from the CD4^{-} or CD4^{+} T cells from WT or AIMP1$^{-/-}$ thymocytes of 11 weeks old mice. cDNA from each population was subjected to semi-quantitative RT-PCR using Foxp3 or HPRT-specific primers. (D) WT CD4^{+} T cells (dotted line) and AIMP1$^{-/-}$ CD4^{+} T cells (solid line) from 11 weeks old mice were analyzed by flow cytometry for the expression of intracellular Foxp3. The data shown are representative of three separate experiments.

Supplementary Fig. 1. Han et al.

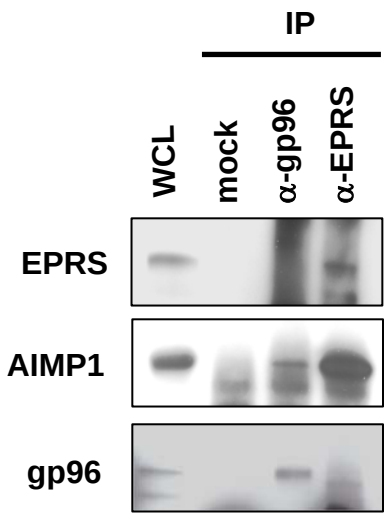

Supplementary Fig. 2. Han et al.

A

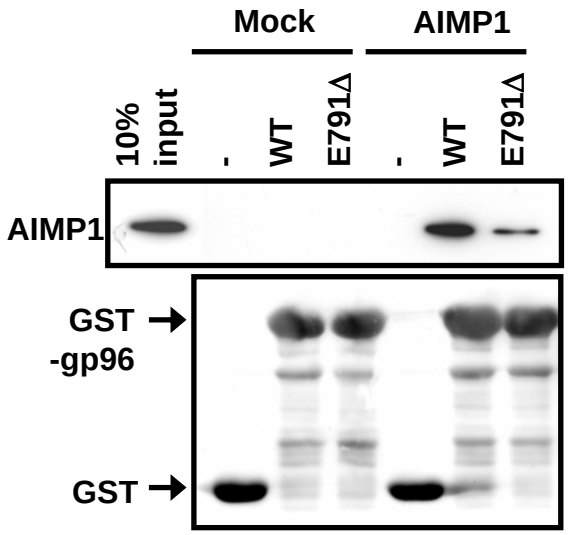

B

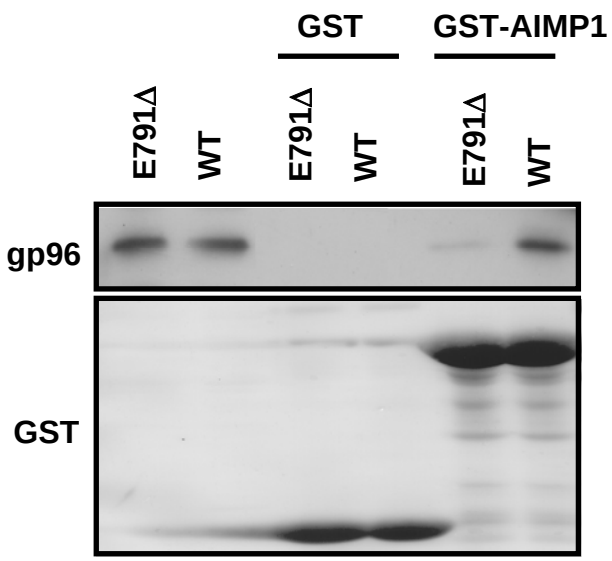

Supplementary Fig. 3. Han et al.

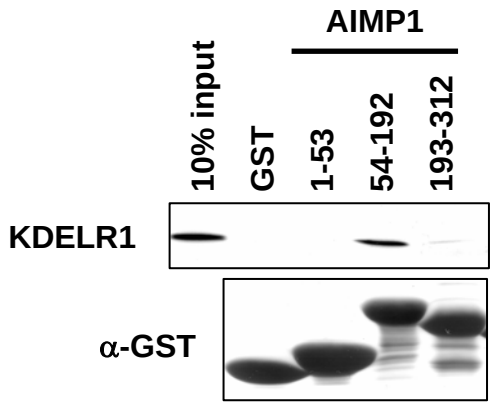

Supplementary Fig. 4. Han et al.

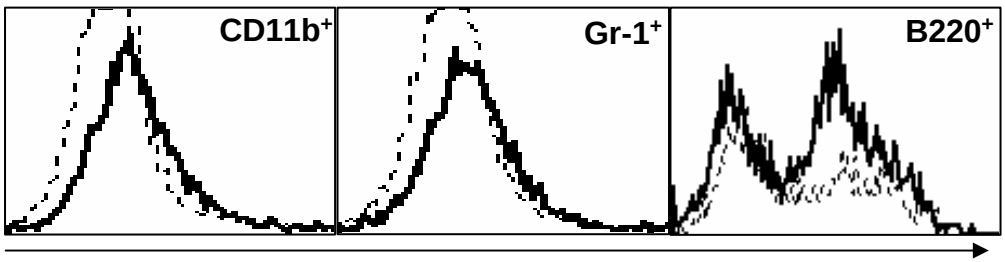

Supplementary Fig. 5. Han et al.

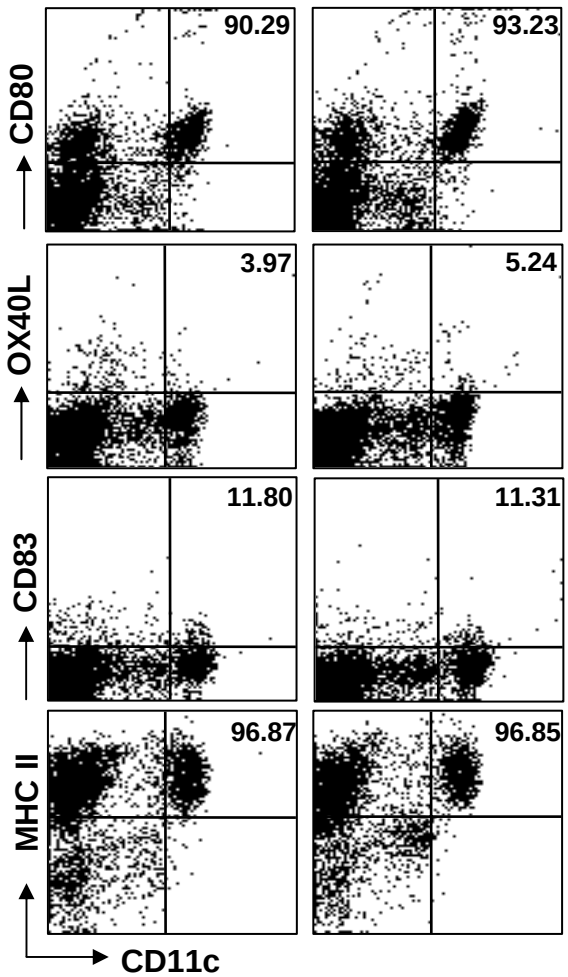

Supplementary Fig. 6. Han et al.